PHOTOVOLTAIC PROPERTIES OF THE GALLIUM ARSENIDE-PEDOT:PSS INTERFACE

by

RICHARD CHARLES CRAMER

A THESIS

Presented to the Department of Chemistry
and the Robert D. Clark Honors College
in partial fulfillment of the requirements for the degree of
Bachelor of Science

July 2014

An Abstract of the Thesis of

Richard Charles Cramer for the degree of Bachelor of Science
in the Department of Chemistry to be taken July 2014

Title: Photovoltaic Properties of the Gallium Arsenide-PEDOT:PSS Interface

Approved: _____

Shannon W. Boettcher

This thesis reports studies on the interface between GaAs and the conductive polymer poly(3,4-ethylenedioxythiophene):poly(styrenesulfonate) (PEDOT:PSS) in a planer Schottky diode architecture. The temperature dependence of the Schottky barrier height of the GaAs-PEDOT:PSS junction was found to be most accurately modeled using an interfacial layer model indicating that an oxide layer is forming at the interface. It has been found that chalcogenide passivation layers deposited from solution onto the GaAs surface did not improve device performance indicating that the passivation layer does not survive the PEDOT:PSS deposition. Small increases in pH of the PEDOT:PSS solution caused by the addition of NH_4OH have been found to increase the fill factor of GaAs-PEDOT:PSS devices slightly, likely due to physical rearrangement of the polymer chains.

Acknowledgements

I would like to thank Professor Shannon Boettcher for his mentorship and for giving me a place in his lab, Andy Ritenour for being my primary graduate student mentor and teaching me everything I know about gallium arsenide, Professor Mark Lonergan for letting me use the environmental control system in his lab and Donald Clayton for his assistance in operating said system. I would like to thank the Beckman Scholars Program for funding this project. I would like to thank my parents Charles and Linda Cramer for moral and financial support throughout my undergraduate career, as well as my sisters and my friends, particularly Madison Cuneo, Nicholas Lovell, and the entire Boettcher Lab. To everyone who helped me with this thesis thank you.

Table of Contents

List of Figures

List of Tables

Introduction

Motivation

Powering our planet is one of the largest scientific and engineering challenges facing the global community. Humans currently use about 18 TW of power and will need an estimated 27 TW by 2040[1]. A diminishing oil supply and the looming threat of global warming have increased interest in renewable energy technologies; wind, hydro, geothermal, and solar. Of these renewable technologies, solar is the only one which has the potential to meet the global power demand. The total power generating potential of solar energy is ~120,000 TW[2], however in order to have solar provide a more significant portion of our power technological advancement is necessary.

Gallium arsenide is a material of interest for photovoltaic applications because it has excellent properties for absorbing the solar spectrum. These properties have been used to make the most efficient single junction solar cells to date, $\eta = 28.8\%$, using GaAs as the absorbing material.[3] It has been shown that nano-structuring the absorbing material in a photovoltaic device can increase efficiency relative to planar devices.[4,5] This motivates research on testing different nano-structuring techniques on GaAs with the goal of maximizing efficiency.[6] One procedural issue that arises when testing nano-structuring is that it can be difficult and expensive to form a conformal transparent junction with the GaAs which is necessary to test device performance. An ideal test junction would be low-cost, low-temperature, air-stable, quick to apply, and would have a well characterized impact on the device performance.

One method that has been used to test nano-structured GaAs is forming a junction with the conductive polymer poly(3,4-ethylenedioxythiophene):poly(styrenesulfonate) (PEDOT:PSS).[7,8] PEDOT:PSS is a conjugated copolymer which is conductive, air-stable for short periods (over hours PEDOT:PSS absorbs water from the air and loses conductivity) and transparent to much of the visible spectrum (Figure I).[9]

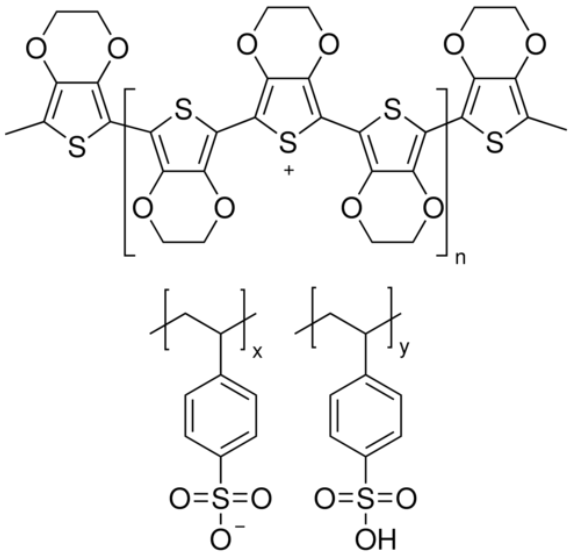

Figure I: PEDOT:PSS

PEDOT is the top copolymer, the conjugated π system allows for conductivity. PSS is the bottom copolymer it functions as a counter ion which allows the PEDOT to be dissolved in water.

The aforementioned properties of PEDOT:PSS mean that it is capable of forming a photovoltaic Schottky junction with GaAs.[7,8] The property that makes it of particular interest is it's solution process ability. PEDOT:PSS is purchased as a suspension in an aqueous solution. Forming a conductive PEDOT:PSS layer is as simple as depositing this solution onto GaAs and driving off the water with heat.[10] This method of deposition is low temperature (~100° C) and does not require a vacuum

system, in this work deposition took an average time of fifteen minutes. Overall using a PEDOT:PSS junction to test GaAs nano-structuring meets the requirements of being low-temperature, air-stable, and quick. Additionally while PEDOT:PSS would likely be too expensive for industrial application the cost of research quantities is not prohibitive. The major remaining question is what are the properties of the GaAs-PEDOT:PSS interface. However while there have been reports of nano-structured GaAs-PEDOT:PSS devices there has been little characterization of the basic properties GaAs-PEDOT:PSS junction.

Most modern electronic devices are made with inorganic materials because of their well characterized and controllable electronic properties. Generally organic electronics do not perform as efficiently as inorganic devices however they are often lighter and more flexible than their inorganic counterparts which makes them preferred for some applications. There is interest in combing the high efficiency of inorganic materials with the flexibility of organic materials; this is the field of inorganic-organic heterojunction devices. This field of research has potential applications for photovoltaics, transistors, lighting, displays, and other electronic devices. Understanding the basic properties of inorganic-organic heterojunctions is a fundamental step in developing this scientific field.[11]

This thesis reports the results of studies which characterize the GaAs-PEDOT:PSS interface in the most basic type of photovoltaic device architecture, the planar Schottky diode. The characterization of the junction in this simple device architecture will provide insight on past research where PEDOT:PSS-GaAs junctions were used to quickly test GaAs nanostructure and will inform any future research which

uses this testing method. Additionally this research illuminates issues for controlling the charge separation at an inorganic-organic heterojunction and demonstrates modification of electrical properties of a solution deposited polymer via solvent changes and ion addition. These results may inform future works in the field of inorganic-organic heterojunction electronic devices.

Background: Photovoltaics[12]

Conventional solar cells work by absorbing sunlight and transferring this energy to excited electrons. Due to the materials used in the solar cell, these energetic electrons flow predominantly in one direction. The average energy that each of these electrons has corresponds to the voltage of the cell. The rate at which electrons leave the cell is the cell's current. Current multiplied by voltage gives the rate of energy output for the cell, the electrical power.

A major result of quantum physics is that bound particles, such as electrons within a material, have quantized energy states rather than a continuous set of allowed energies. For example consider an electron bound within a solid which has some negative energy measured in electron volts (eV) where zero is the energy required for the electron to leave the solid. Classically the electron can have any energy and can gain or lose energy in any amount, (Figure II A. Classical). If however the allowed energy states are quantized to only integer energies then the electron must have an integer energy and it can only gain or lose energy in integer multiples of eV (Figure II B. Quantized). For extended solids such as the semiconductor GaAs, the allowed energy states are clustered in bands where within the band there are so many states that it can be assumed that there is a continuous distribution and outside the bands there are no

states. An electron can gain or lose energy only in amounts that leave the final energy within a band, (Figure II C. Band Structure).

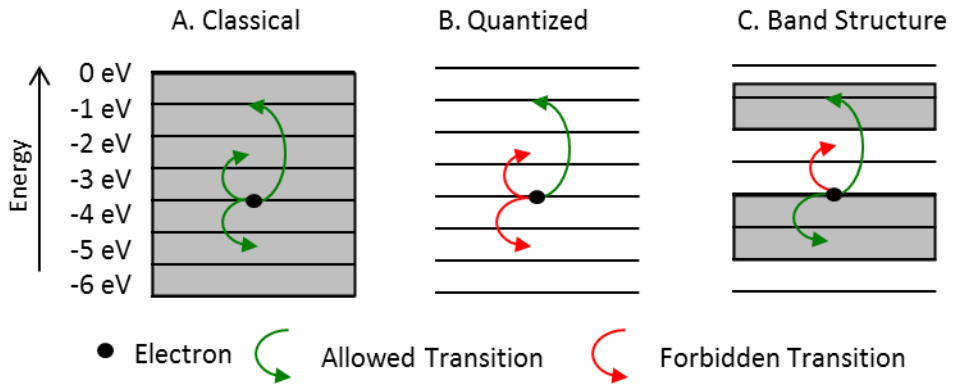

Figure II: Energy quantization and band structure

(A) Classically an electron can have any given energy and can gain or lose energy in any amount. (B) If the energy states were quantized to integer values an electron would necessarily have an integer value of energy and could only gain or lose energy in integer multiples. (C) In an extended solid the allowed energy states cluster in bands, represented in gray, an electron necessarily has energy within a band and can only gain or lose energy in amounts that leave it in a band after the transition.

Electrons are fermions meaning that no two electrons can occupy the same overall state. Because bands have a finite number of states within them they can only have a finite number of electrons, this means that bands will fill up. Semiconductors are materials which have a band which is completely filled with electrons and another band above the first which is close enough in energy that random thermal excitation can excite an electron from the top of the filled band to the bottom of the empty band. The highest band which has electrons filling most of the states is called the valence band and the next band up in energy which is almost empty is called the conduction band. The

energy difference between the top of the valance band and the bottom of the conduction band is called the band gap (E_g), (Figure III left).

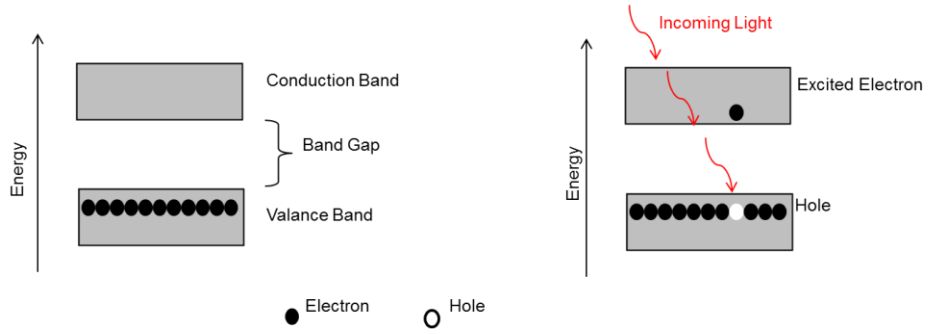

Figure III: Band structure and electron-hole pair generation

(left) This is a band structure, the vertical axis is in energy, the horizontal axis is in space. Electrons can have any energy in either the valance or the conduction band represented by gray bars. Between these bands is a set of energies that an electron cannot have called the band gap. For semiconductors the valance band is almost full and the conduction band is almost empty (right) This figure shows the excitation of an electron from the valance band into the conduction band of a semiconductor. The state from which the electron was excited from becomes a mobile hole.

Sunlight is composed of quantized packets of energy called photons. The energy of a photon is dependent upon its frequency; high frequency photons have high energy, low frequency photons have low energy. Photons which have energy equal to or greater than the band gap can be absorbed by an electron in the conduction band and promote it into the valence band, photons which have energy less than the band gap cannot be absorbed because there is no state between the valance and conduction band for the electron to go to. When an electron is promoted from the valance to the conduction band this creates what is known as an electron-hole pair. An electron-hole pair consists of an electron with extra energy in the conduction band and the unoccupied energy state which that electron left behind in the valance band called a hole. Because electrons can

move between spatial states of the same energy freely, and the valence band is otherwise filled with electrons, the hole is mobile and can be treated like a particle with a positive charge. This is analogous to the concept of a bubble in a liquid, though it is actually the liquid which is moving it is easier to describe the motion of the bubble (Figure III right).

The first limiting factor of solar cell technology is the band gap of the absorbing material. A semiconductor can only absorb photons which have energy equal to or greater than its band gap. The maximum amount of energy that can be extracted from an excited electron is correlated to the band gap energy; all excess energy is dissipated as heat. Thus there is a balance between absorbing a large number of photons and getting more energy per photon. This fundamental limitation, when combined with the solar spectrum gives the theoretical Shockley-Queisser limit for efficiency (Figure IV).

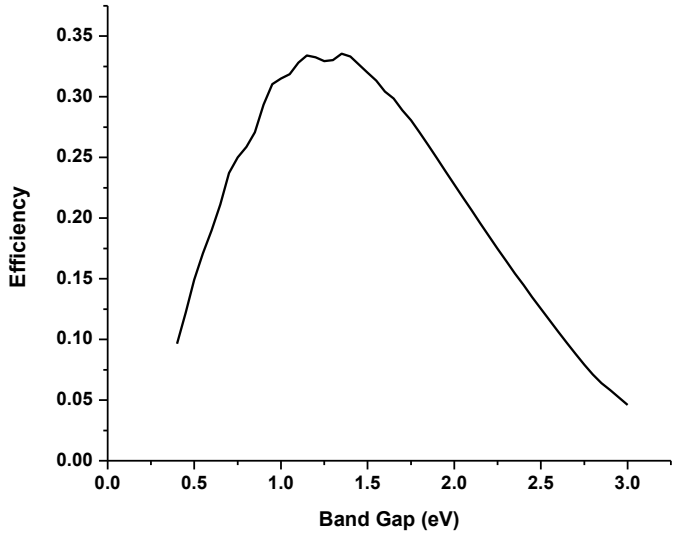

Figure IV: The Shockley-Queisser limit.

This figure shows a first approximation of the theoretical limit for efficiency single junction photovoltaic device as a function of band gap. For reference Silicon has a band gap of 1.1 eV and gallium arsenide has a band gap of 1.42 eV.

Normally electrons transition to the lowest energy state possible by dissipating the energy they have as heat. However, the rate at which the electron makes the transition and releases energy is inversely correlated to the amount of energy being released. There are an almost continuous set of states within a band so transition times within a band are very small, this means that an electron which absorbed a highly energetic photon, and is therefore in a highly energetic state in the conduction band, will quickly release energy as heat until it is at the bottom of the conduction band. Conversely the amount of energy which the electron would need to release in order to cross the band gap is large and therefore the transition from the valance band to the conduction band does not occur at a rapid rate. If we design the system such that the electron and the hole move in opposite spatial directions before there is enough time for

them to recombine then we have prevented the recombination from happening at all because the energetic electron and the hole now no longer occupy the same special region. This separation of the electron hole pair is accomplished at a junction between two materials.

In a photovoltaic device the absorbing semiconductor layer is placed in electrical contact with another material with different average electron energy to form a junction. The average electron energy is called the Fermi-level. In these experiments the semiconductor GaAs is placed in contact with the conductor PEDOT:PSS which has a lower Fermi-level. The bulk Fermi-levels of the two materials equilibrate until the potential difference generated by moving electrons from one region to another cancels the initial potential energy difference between the two materials. For n-type semiconductors such as the n-GaAs used for this thesis, this results in the energy states at the interface being higher than the energy states in the rest of the semiconductor (Figure V).

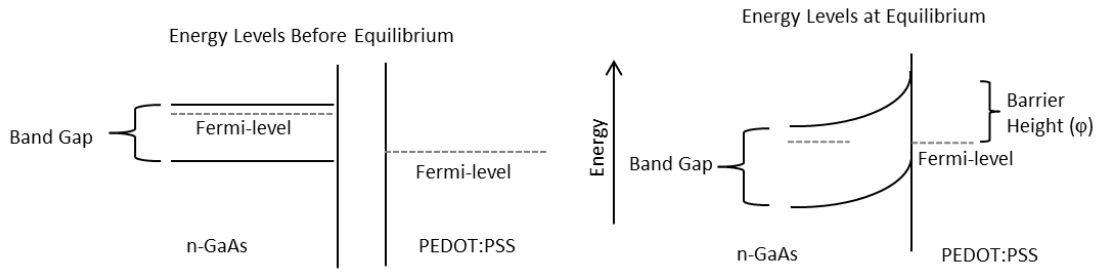

Figure V: Band bending diagram at equilibrium

In this figure the gray bands from Figure I have been replaced with lines representing the top of the valance band and the bottom of the conduction band. The vertical lines represent the physical edge of the materials. The Schottky barrier height (φ), a metric for measuring band bending, is indicated on the right.

Electrons or holes which are generated in the region of space where the bands are bent or ones which diffuse into that region will have a preferential movement; the electrons will flow down in energy into the semiconductor while the holes will rise in energy into the metal. This separates electron-hole pairs generated by the absorption of photons and gives us useful current, (Figure VI). This current is called the photocurrent.

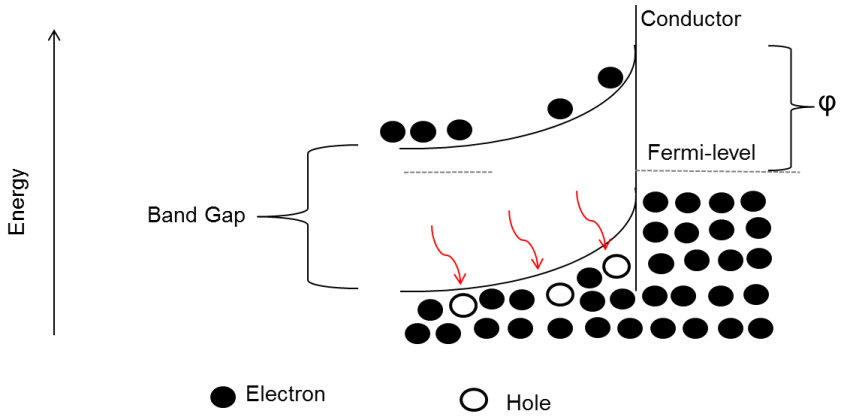

Figure VI: Electron-hole pair separation

Photogenerated electron-hole pairs in the bent band region flow with a preferential direction, elections flow downhill to the left, holes flow uphill to the right. In n-GaAs there are already a large number of electrons in the conduction band so the limiting part of the photocurrent comes from the holes moving into the conductor. Electron hole pairs generated away from the bend band region will contribute to photocurrent only if the hole drifts into the bent band region.

When the circuit is completed the voltage generated is directly correlated to the energy structure at equilibrium (Figure V right), particularly the amount of band bending which can be characterized by the Schottky barrier height (φ) defined as the difference in energies between the Fermi-level of the conductor and the conduction band edge of the semiconductor at the interface. This value expresses the potential barrier over which electrons would need to flow to go from the semiconductor into the conductor, the opposite direction of the photocurrent. The Schottky barrier also serves

as an upper bound for the maximum voltage which we can expect to get out of the cell. To understand a new system like GaAs-PEDOT:PSS it is important to characterize the barrier height and seek out ways to understand the fundamental chemical and physical interface parameters that controls it's magnitude.

To characterize the devices there are three common tests, light current voltage measurements, dark current-voltage measurements, and impedance-voltage measurements. We will use each of these measurements to obtain estimates of the Schottky barrier height for our devices. Each of these measurement techniques and their interpretations will be discussed in the results section.

Background: Materials

With an understanding of basic photovoltaics we can now characterize why gallium arsenide is a good absorbing layer. Gallium arsenide has a band gap of 1.42 eV which puts it near the top of the curve for theoretical maximum efficiency (Figure IV). Gallium arsenide also has a high absorption coefficient meaning that it can absorb a large number of photons in a thin layer of material, 95% absorption in 1×10^{-6} m.[12]

A major obstacle for gallium arsenide technology is that it readily reacts with oxygen to form an oxide layer at the surface. This oxide layer introduces states in the middle of the band gap at the surface, this increases recombination of electron-hole pairs at the surface and reduces photocurrent. This also reduces the voltage of the cell by reducing the overall energy difference between the holes and electrons which are separated. It has been shown that treating the gallium arsenide surface with chalcogenides, particularly sulfur compounds, can decrease electron hole pair recombination at the GaAs surface relative to an untreated surface. Sodium sulfide,

sodium hydrosulfide, and alkanethiols have all been shown to effectively passivate the GaAs surface. [13, 14, 15] Hypothetically this is caused by prevention of the formation of an oxide layer.

PEDOT:PSS films are generally deposited from an aqueous solution however studies have been performed to determine how altering the solution chemistry changes the properties of the resultant film. It has been found that the addition of large organic solvents such as ethylene glycol to an aqueous PEODT:PSS solution increase the conductivity of the resultant film. It is hypothesized that this is due to a physical rearrangement of the polymer chains caused by the change in solvent polarity.[16] It has also been found that the addition of anionic surfactants increases conductivity, this is again attributed to a physical rearrangement of the polymer chains.[17]

Experimental

Methods

Devices were made from wafers of (100) n-type GaAs doped with silicon, N_d = 6.9×10^{16} - 2.0×10^{17} cm^{-3}, (Wafertech) cut to ~0.025 cm^2. Ohmic back contacts were formed by thermally depositing 100 nm of 80/20 Au/Ge alloy and annealing at 450° C for 120 s in forming gas (95% nitrogen 5% hydrogen). The wafers were mounted to glass slides using silver paint (Ted Pella), which provided the back contact. Chemically resistant epoxy (EpoTec) was used to secure the wafer and isolate the conductive path to the back contact. The GaAs was rinsed with isopropyl alcohol, ethanol, and water then etched for 30 s in a solution of (1:1:50) conc. H_2SO4: 30% H_2O_2:H_2O. The GaAs was rinsed with water for 10 s then dried with nitrogen. If a chemical passivation experiment was being performed the GaAs was then submerged in a solution of passivating agent then dried with nitrogen again. 5 µl of a mixed PEDOT solution was drop cast onto the GaAs and the device was cured for 12 minutes at 100° C under nitrogen. The mixed PEDOT solutions were one part PEDOT:PSS 5 wt % high-conductivity grade (Sigma Aldrich), two parts ethylene glycol, and one part a solution that was either pure water or an aqueous solution of NH_4OH or NH_4Cl. For a top contact silver paint was applied to part of the PEDOT:PSS layer which did not overlap the GaAs,

Room temperature measurements were performed in a nitrogen atmosphere using a BioLogic potentiostat. Temperature dependent measurements were performed in a liquid nitrogen cooled environmental chamber (Sun) using a Keithly 236 source-meter

unit and a Soltron impedance analyzer. Illumination was provided by a ThorLABs M660L2 LED which was adjusted to a produce a constant photocurrent for each device, 10 mA cm^{-2} for room temperature tests and 3 mA cm^{-2} for temperature dependent measurements.

Temperature Dependent Measurements

To fully characterize the interface between gallium arsenide and PEDOT:PSS we performed a series of temperature dependent measurements. We tested the capacitance-voltage response in the dark and the current-voltage response both in the dark and under illumination normalized to give 3 mA cm^{-2} photocurrent at zero applied bias. All measurements were repeated over a temperature range of 150 K to 290 K. We then compare the data from these tests to different models of charge transport and extrapolate values for the Schottky battier height of the junction. Data will be shown for a characteristic sample.

Light current-voltage measurements simulate normal operating conditions; this is similar to the process described in the background section except a voltage is applied to simulate a load on the device. In the band diagram this can be thought of as unbending the bands. This drives current from the conductor into the semiconductor, the opposite direction of the photocurrent. The behavior of a Schottky diode under applied bias and without illumination is described with the ideal diode equation, (Equation I).

$$\text{Equation I:} \qquad J = J_o \, e^{\frac{qV}{nkT}} - 1$$

In the ideal diode equation the measured current density *J* is dependent upon the controlled variables of voltage *V* and temperature *T* and the constants of the dark

saturation current density J_o, the electron charge q, and Boltzmann's constant k. The n in the exponential is called the ideality factor and is a measure of how close the data matches the ideal diode which would have an ideality factor of one. The dark saturation current is the amount of current which flows from the conductor into the semiconductor with zero applied voltage, (Figure VII).

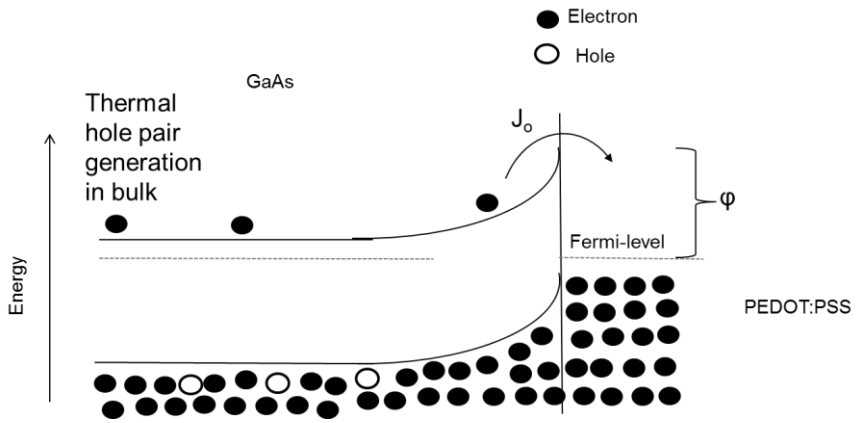

Figure VII: Dark saturation current density

Thermal excitation can create electron hole pairs that move randomly. While the potential field generally moves electrons to the left some thermally excited electrons will have enough energy to move over the barrier height (φ) into the conductor. This is called the dark saturation current density J_o and is dependent on the temperature and the barrier height. Note that while electrons move from left to right the current flows from right to left.

For this study the important values from the light current-voltage data are the open circuit voltages, V_{oc}. These are measures of the maximum voltage that the device can produce. This correlates to the point where the current from the applied bias cancels out the photocurrent, J_{ph}, (Equation II).

Equation II: $$V_{oc} = \frac{nkT}{q}\left(\ln\frac{J_{ph}}{J_o} + 1\right)$$

Note Equation II is Equation I solved for V when $J = J_{ph}$. In Figure VIII this can be seen as the points where the light curves cross the zero current axis.

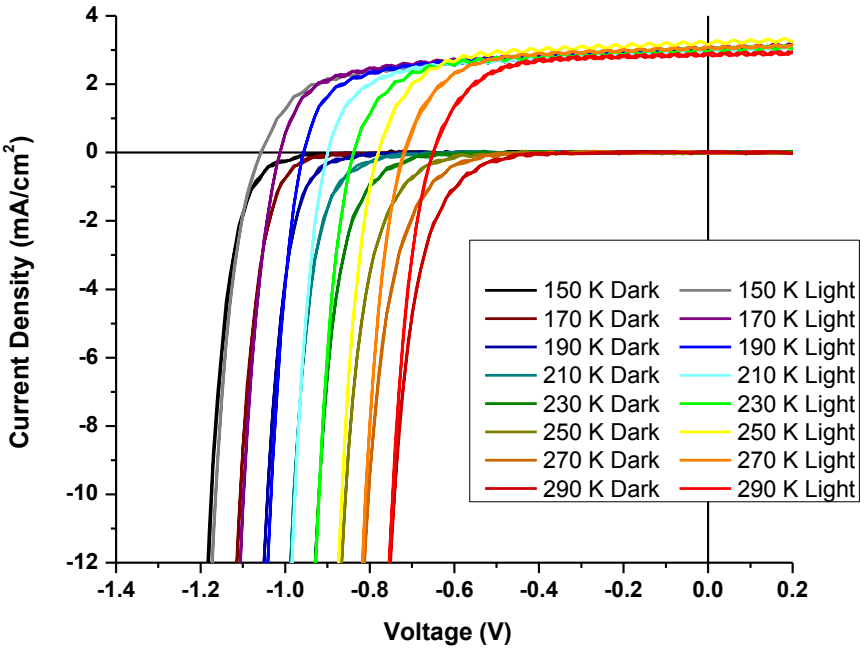

Figure VIII: Light and dark current-voltage curves from 150 K to 290 K

The lower temperature tests (left) have a higher V_{oc} and a reduced fill factor compared to the devices closer to room temperature (right).

It can immediately be observed in Figure VIII that the open circuit voltage of the devices is increasing in magnitude with decreased temperature. This is expected from Equation II. This gives us a lower bound for what the barrier height actually is in these devices as a function of temperature.

Another metric for interpreting light current-voltage data is the fill factor, qualitatively this is how square the curve is. A squarer curve has a higher fill factor this means that the device is providing more photocurrent over a larger voltage range and that overall the device is more efficient. The fill factor correlates to the resistivity and

the undesired electron-hole recombination rates in the device, if either are high than the fill factor will be low. When fit to the ideal diode equation a low fill factor is reflected by the ideality term being higher than one

From the dark current-voltage measurements shown in Figure VIII we can determine the dark saturation current and the ideality by plotting the natural log of the current verses the voltage (Figure IX) and performing a linier fit to a rearranged ideal diode equation (Equation III).

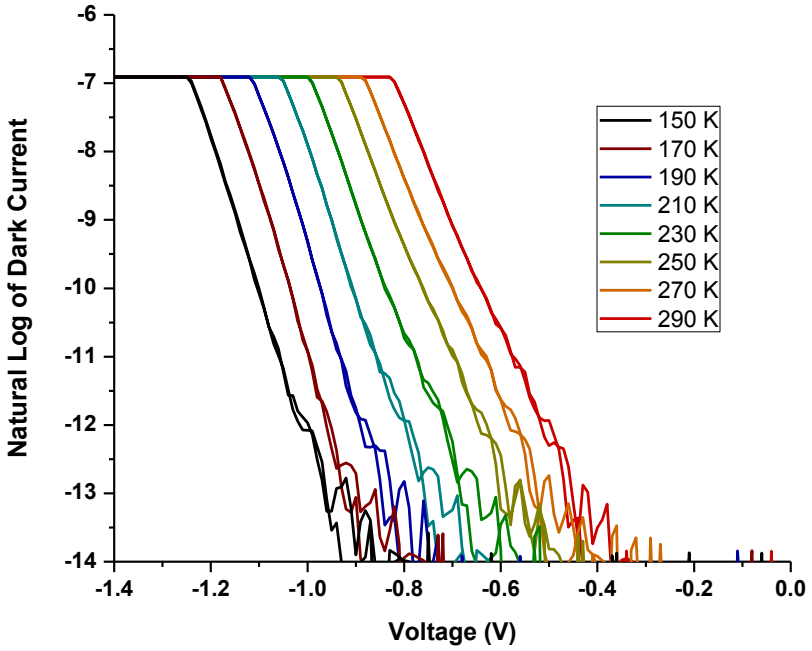

Figure IX: log of current versus voltage

By fitting the linear region of this ln(I) vs V plot to Equation III we extrapolate values for the dark saturation current J_o and the ideality n at each temperature.

$$\text{Equation III:} \quad \ln J = \ln J_o + \frac{V}{nkT}$$

The dependence of the barrier height of the dark saturation current is given by thermionic emission theory (Equation IV).[11, 18]

$$\text{Equation IV:} \quad J_o = \kappa A^* T^2 e^{\frac{-q\varphi^{TE}}{kT}}$$

κ is a transmission probability for electrons with sufficient energy to cross the barrier, assumed to be 1, and A^* is the Richardson constant 8 A cm^{-2} K^{-2} for GaAs.[19]. The barrier height as determined by this method is φ^{TE}, where TE designates thermionic emission theory.

Impedance-voltage curves were also collected over the same range of temperatures. The capacitance of the devices comes from the charge separation which occurs when the two materials equilibrate. In this experiment we apply both a DC and an AC bias to our devices and extract out a value for impedance. This experiment is performed without illumination. By selecting data from the AC frequency regime such that the phase difference between the input and output signals is ~90° we select a region where the impedance can be considered entirely capacitive. In such a region we can fit the data to the Mott Schottky model which follows the equation,[11, 18]

$$\text{Equation V:} \quad C^{-2} = \frac{2(\varphi^{CV} - V_p - V - \frac{kT}{q})}{\mathrm{q}\,\varepsilon_s\, N_d\, A^2}$$

where C is the capacitance, ε_s is the permeability of GaAs, 1.1 ×10^{-10} m^{-3} kg^{-1} s^4 A^2 [12], N_d is the dopant density, A is the device area, and V_p is the distance between the Fermi level of the GaAs and the bottom of the conduction band

$$\text{Equation VI:} \quad V_p = \frac{kT}{q} \ln \frac{N_c}{N_d}$$

where N_c is the effective density of states in the conduction band 4.70 ×10^{17} cm^{-3}. The barrier height calculated by this method is φ^{CV}, CV indicating that this was calculated

from the capacitance voltage measurements. This data is analyzed via a Mott-Schottky plot where C^{-2} vs V is plotted and a linear fit is performed (Figure X).

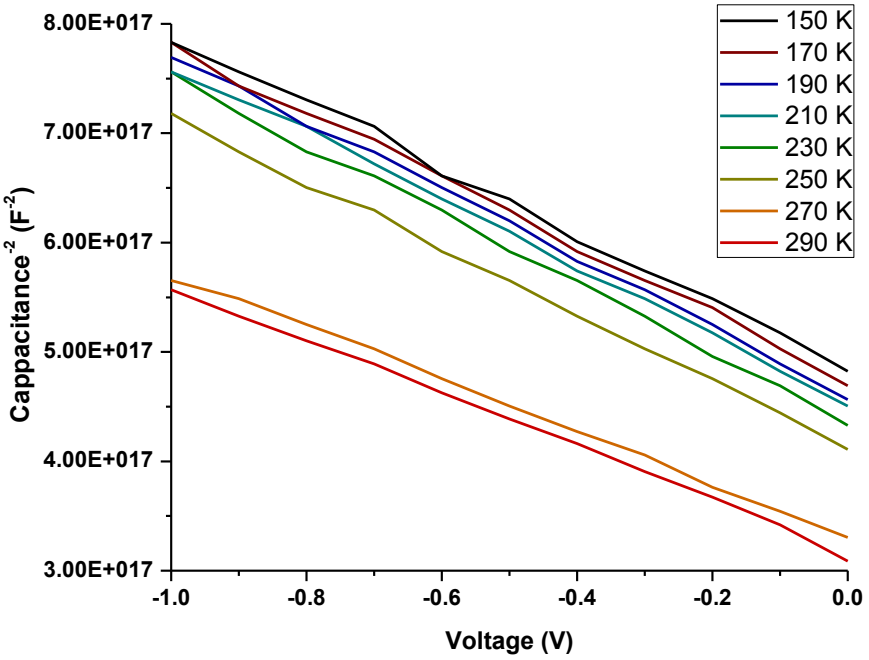

Figure X: Mott-Schottky plots at a range of temperatures

By fitting this inverse squared capacitance vs voltage data to the Mott-Schottky relationship (Equation III) we can calculate values for the barrier height and dopant density.

Fitting this data gives us our second value for the barrier height and a set of dopant densities from which we can determine how accurate our modeling is (Table I), we see that our calculated dopant densities are slightly lower than what the GaAs manufacturer specifies (4.70×10^{17} cm^{-3}) but are the right order of magnitude which indicates that we have an acceptable fit.

	Capacitance-Voltage Results			Current-Voltage Results			
T (K)	N_d (cm^{-3})	φ^{CV} (eV)	φ^{IL} (eV)	J_o (mA/cm^2)	n	φ^{TE} (eV)	$\lvert V_{oc}\rvert$ (V)
290	6.14×10^{16}	1.33	0.845	3.02×10^{-08}	2.33	0.769	0.650
270	5.94×10^{16}	1.44	0.905	1.64×10^{-08}	2.58	0.727	0.715
250	4.88×10^{16}	1.42	0.891	3.45×10^{-09}	2.67	0.703	0.780
230	4.58×10^{16}	1.42	0.863	1.13×10^{-10}	2.54	0.711	0.835
210	4.38×10^{16}	1.56	0.967	3.73×10^{-12}	2.50	0.708	0.895
190	4.28×10^{16}	1.55	0.943	2.76×10^{-13}	2.62	0.680	0.955
170	4.18×10^{16}	1.60	0.948	5.99×10^{-14}	2.92	0.628	1.02
150	4.09×10^{16}	1.65	0.976	2.42×10^{-14}	3.39	0.562	1.06

Table I: Derived values from temperature dependence experiments

These values correspond to a single device selected to be characteristic representation of all measured samples.

Since our ideality factors from the fit of the ideal diode equation are over one we know that we have significant deviation from the ideal diode model. To account for this we combine the information from our dark current voltage and impedance voltage data and compare it to the interfacial layer model.[11, 18] This model describes deviations from thermionic emission theory by proposing that there is a thin insulating layer at the interface that has a density of states in the band gap, which may be a suitable model for an interfacial oxide layer in this system. The interfacial layer model proposes that an adjustment should be made to the barrier height calculated from the capacitance voltage, φ^{CV}, such that

Equation VII: $$\varphi^{IL} = \varphi^{CV} - \varphi^{cor}$$

Equation VIIII: $$\varphi^{cor} = (1 - \frac{1}{n})^2(\varphi^{CV} - V_{avg} - V_p - \frac{kT}{q})$$

where φ^{cor} is the correction made to φ^{CV} to get the corrected interfacial layer model barrier height φ^{IL}, V_{avg} is the average values of applied bias over which n and J_o were calculated from the ideal diode equation fitting, Equation I. The relevant results from all temperature dependent measurement experiments are displayed in Table I and Figure XI.

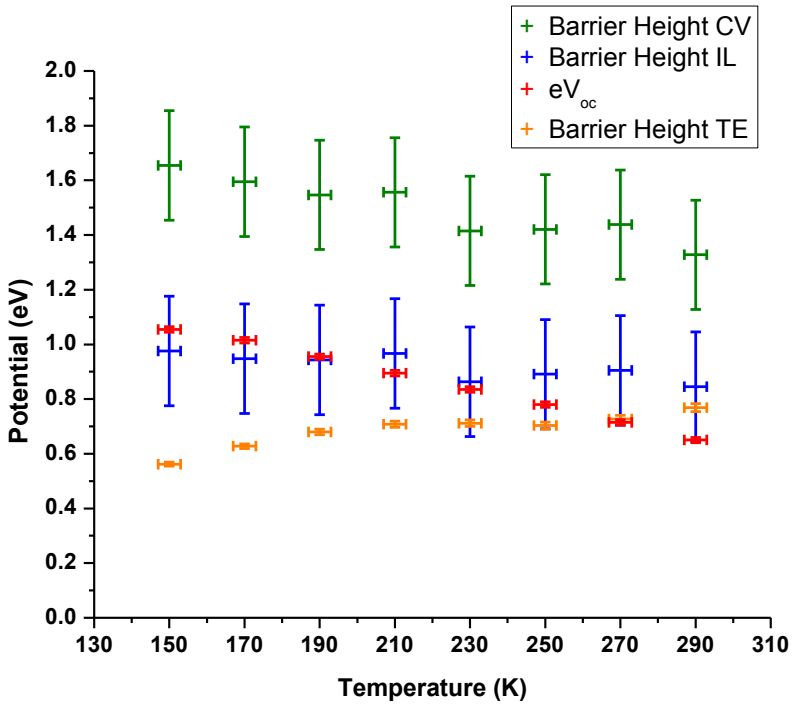

Figure XI: Comparison of barrier height temperature dependence

This figure shows values of the barrier height calculated by the four different methods, the width and height of the crosses shows the error. These values correspond to a single device selected to be characteristic representation of all measured samples. Note eV_{oc} is not a measure of the barrier height but rather the open circuit voltage multiplied by the electron charge. We would expect the actual barrier height to be ~0.1-0.5 eV above eV_{oc}.

Comparing our values for the barrier height we can see that thermionic emission theory barrier heights are below the open circuit voltage, which is not reasonable. The

capacitance voltage data gives us high but physically possible (within error) values. The barrier height should be typically a few hundred mV above the open circuit voltage and below the band gap of GaAs,[11, 20] note the band gap increases as we decrease temperature to a value of ~1.5 eV at 150 K. The interfacial layer model gives the best fit to the actual V_{oc} data. From this we can hypothesize that there is an interfacial layer. Since it is known that oxides form readily on the GaAs surface we hypothesize that this is an oxide which formed during or after deposition of the PEDOT:PSS layer. Despite this interfacial layer the voltages which we see are adequate for using PEDOT:PSS as a laboratory testing technique. Though the exact properties of the interfacial layer would still need to be characterized and controlled.

NH_4OH Addition to PEDOT:PSS

To prevent the formation of the oxide layer on the GaAs surface we will try chalcogenide passivation. As discussed in the introduction studies suggest that chalcogenide passivation prevents the formation of an oxide layer. It is known that sulfur containing compounds react with acids to form hydrogen sulfide gas. This would remove the sulfide layer from the GaAs and prevent passivation. Unfortunately PEDOT:PSS is acidic. We would like to chemically control the pH of the PEDOT:PSS solution with the end goal of neutralizing the PEDOT:PSS solution without significant negative impact on device performance.

To test the effect of pH on the performance of devices a set of PEDOT:PSS solutions of 1/1/2 PEDOT:PSS/X/ethylene glycol were prepared with X being NH_4OH solutions of varying concentration. Ethylene glycol was added because it has been shown to increase the conductivity of PEDOT:PSS films this resulted in five

PEDOT:PSS solutions; 0 mM, 1.25 mM, 2.5 mM, 5 mM, and 10 NH_4OH. These correspond to final solution pHs of 2.33, 2.43, 2.70, 6.90, and 11.43 respectively. Devices were made using these solutions and current voltage curves were taken (Figure VI).

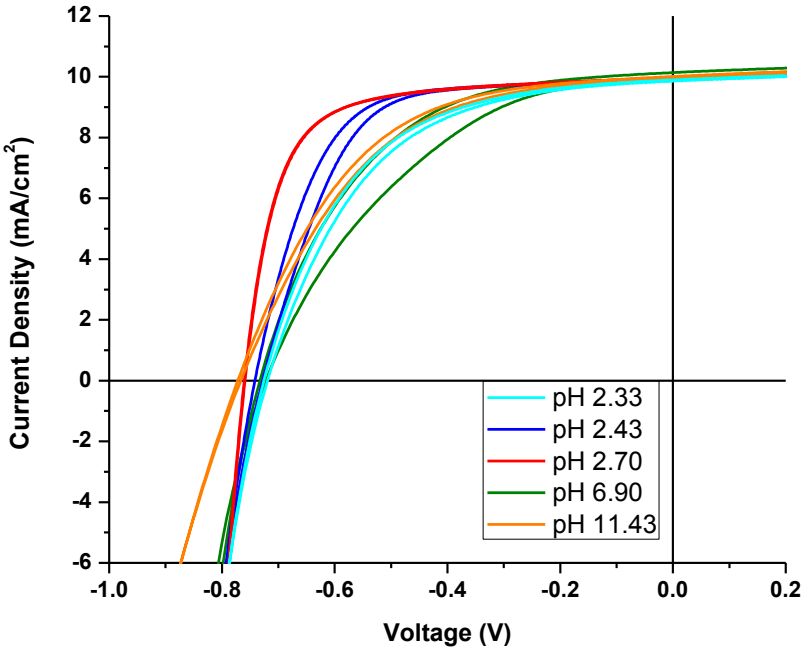

Figure XII: Comparison of devices with NH_4OH modified PEDOT:PSS

PEDOT:PSS films made from pH 2.43 and pH 2.70 devices resulted in higher fill factors than unmodified PEDOT:PSS solutions (pH 2.33). Further addition of NH_4OH decreased this effect. The change in V_{oc} is not statistically significant over multiple samples

The devices made with 1.25 mM of NH_4OH and 2.5 mM NH_4OH exhibited a small improvement in fill factor relative to the 0 mM NH_4OH devices, continuing up to 5 mM and 10 mM NH_4OH reduced this effect. To determine if the cause of this change in performance was the change in pH or the addition of ions to the solution this process

was repeated using NH_4Cl solutions. No statistically significant change in performance was observed until 5 mM NH_4Cl at which point the fill factor decreased. This indicates that the presence of Cl^- is an insufficient substitute for OH^- and so in this instance the process is better described as a pH effect.

It has been proposed that the addition of ions can change the morphology of the PEDOT:PSS film by enabling the larger PEDOT copolymer to arrange itself more evenly in space with the smaller PSS chains[17], however if this were the predominant mechanism for the improvement we would expect to see a similar improvement in the NH_4Cl samples which we did not see, though it is possible that the effect was too small to be observed as there was significant variance in the fill factors. For the purposes of this project it was proven that neutralizing the PEDOT:PSS solution still results in a functional device and therefore sulfur passivation can be attempted without the sulfur simply reacting with the acidic solution.

Chalcogenide Passivation

Initial attempts at chalcogenide passivation used a common chemical passivating agent Na_2S. It was found that increased immersion time in Na_2S solution did not significantly increase device performance and that long term immersion reduced device performance (Figure XIII). This reduction in performance is likely caused by the formation of resistive polysulfide chains at the interface.

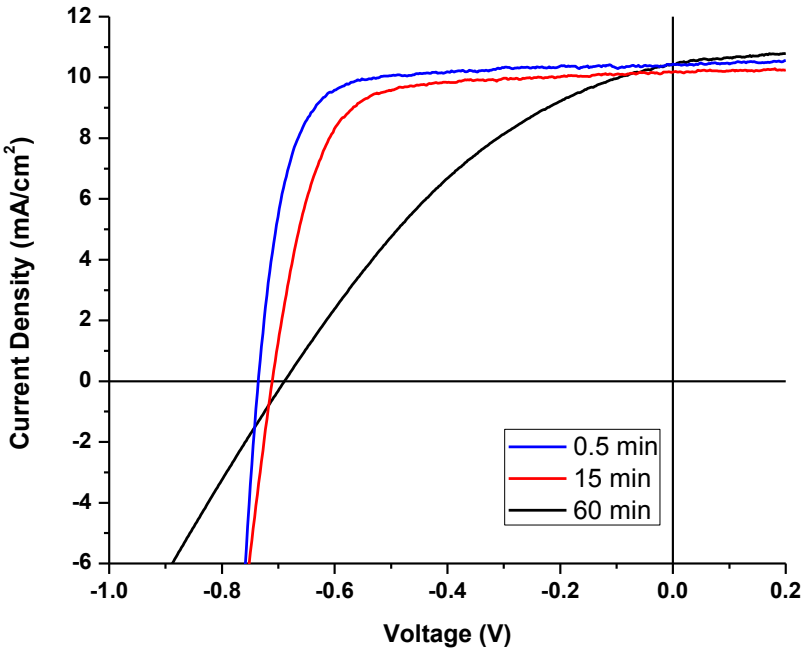

Figure XIII: Effect of immersion time on Na_2S passivation tests

Short immersion times had no significant effect on device performance, long immersion times resulted in significantly increased series resistance as can be seen by the reduction in device fill factor.

Combinations of pH 2.3, 2.7, 6.9, and 11.43 PEDOT:PSS solutions and the chalcogenide passivating agents; Na_2S, NaSH, $C_XH_{2X+1}SH$ (X=3, 6, 12), and $NaSO_3C_3H_6SH$ all failed to increase device performance. Variation of solution concentration from 0.01 M to 1 M, and of submersion time from 5 s to 48 h. All either resulted in no significant effect, a decrease in device performance which could be attributed to an increase in series resistance, or such a significant decrease in performance that devices could not produce 10 mA cm^{-2} of photocurrent. The most efficient curves for each passivating agent came from devices using pH 2.70 PEDOT:PSS (Figure XIV).

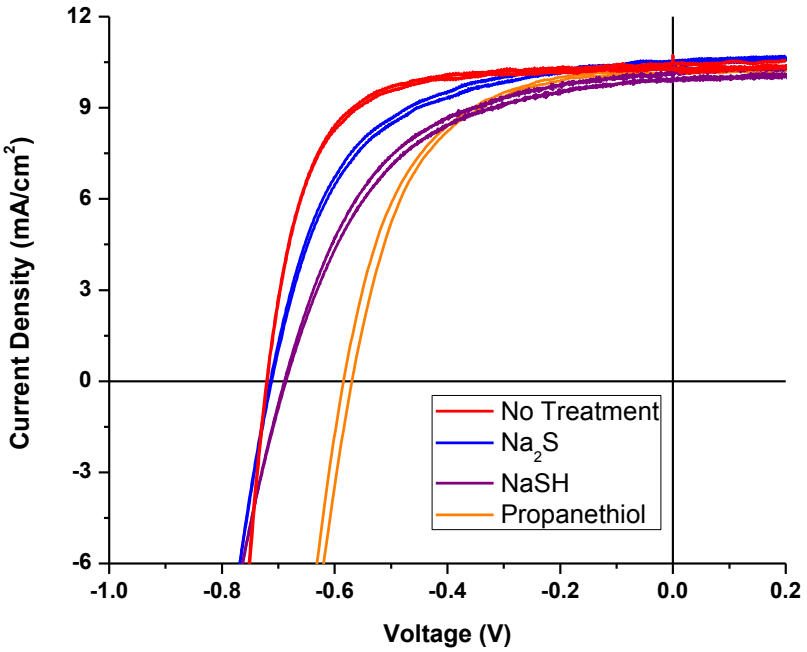

Figure XIV: Most efficient device for each chalcogenide treatment

Each curve was with the shortest immersion time, the least concentrated solution and the with the pH 2.70 PEDOT:PSS. This indicates that the passivating agent is having no performance improving effect and that the dominant factor is the PEDOT:PSS.

The failure of the passivation techniques which are known to work in other architectures indicates that either the PEDOT:PSS has some passivating ability itself which is comparable to the passivating effect of the chalcogenide compounds or that the chemical treatments do not survive the PEDOT:PSS deposition. The second hypothesis seems more likely as the sulfurs in the PEDOT:PSS are spaced far apart on a bulky organic molecule and there would be a large amount of steric hindrance for the sulfurs to reach a significant portion of the surface. Additionally there was no observed effect when changing the pH of the PEDOT:PSS solution. We would expect the less acidic PEDOT:PSS solutions to form better devices than the acidic PEDOT:PSS solutions

because the less basic solutions would not react with the chalcogenides. However the less-acidic PEDOT:PSS solutions resulted in highly resistive films and the addition of any passivating agent resulted in devices unable to generate 10 mA/cm^2 photocurrent at zero applied bias. It seems likely that the water which is the solvent for the PEDOT:PSS is dissolving any small sized passivating chemicals used and that the alkane thiols too large for the water to dissolve are also too large to allow significant current to pass. The bonding strength of the chalcogenides to the GaAs surface appears to be insufficient for the passivating layer to survive PEDOT:PSS deposition.

Conclusion

The temperature dependence measurements indicate that there is an insulating interfacial layer between the GaAs and the PEDOT:PSS. This is an unsurprising result as it is difficult to prevent the GaAs from forming an insulating oxide if there is any air exposure in the manufacturing process. Ideally a passivation step would prevent this oxide from forming. The voltage which we are getting out of the devices despite the oxide layer is good enough for PEDOT:PSS to be a good candidate for experimental use if a way to control the oxide layer in this architecture can be found.

It is likely that the solution processability which makes PEDOT:PSS such a good candidate also means that solution based passivation techniques are difficult to apply as the PEDOT:PSS solution may simply be re-dissolving the thin layers of passivating agent and thick passivating layers which survive this PEDOT:PSS deposition introduce significant resistive barriers and. While this research was being undertaken the Huffaker group out of UCLA found that solution deposited chalcogenide passivation did increase the efficiency of similar devices.[21] A major procedural difference between their work and ours was that the Huffaker group used a spin coating technique to deposit the PEDOT:PSS films whereas we used a drop casting method. The spin coating method of deposition puts the passivation in contact with significantly less PEDOT:PSS solution for a significantly shorter amount of time. Using this method of PEDOT deposition would mitigate the problem of re-dissolving the passivation agent.

The issues of controlling charge transport investigated in this study of the GaAs-PEDOT:PSS system are similar to the issues which are encountered for other inorganic-

organic heterojunction technologies such as perovskite photovoltaics which have recently become prominent in the literature.[22, 23] This research provides an examples of the interface between GaAs and PEDOT:PSS being modeled using standard inorganic semiconductor physics techniques. Further research in this field will help determine when these techniques are suitable and will lead to a greater understanding of inorganic-organic heterojunction electronics.

Bibliography

1. US DOE, international energy outlook, 2014

2. Lewis, Powering the Planet MRS Bulletin, 2007, 32

3. Alta Device, June 20th, 2013. Alta Devices NREL Study Shows Alta Devices Solar Material Retains Exceptionally High Efficiency At Elevated Temperatures And Operates Up To 10 Degrees Cooler Than Silicon In Real-World Conditions. [press release] http://www.altadevices.com/pr-2013-06-20.php

4. Walter, M.; Warren, E.; McKone, J.; Boettcher, S. W.; Qixi, M.; Santori, L.; Lewis, N. S. Solar Water Splitting Cells. Chem. Rev. 2010, 110, 6446-6473

5. Kelzenberg, M. D. et al; Boettcher, S. W.; Petykiewicz, J. A.; Turner-Evans, D. B.; Putnam, M. C.; Warren, E. L.; Spurgeon, J. M.; Briggs, R. M.; Lewis, N. S.; Atwater, H. A. Enhanced absorption and carrier collection in Si wire arrays for photovoltaic applications. Nat. Mater., 2010, 9, 239-244

6. Ritenour A.J., Levinrad S., Bradley C., Cramer, R.C., Boettcher S.W., Electrochemical Nanostructuring of n-GaAs Photoelectrodes, ACS Nano, 2013, 7 (8), 6640-9

7. Chao J. J., Shiu S.C., Hung S.C., Lin C.F., GaAs nanowire/poly(3,4-ethylenedioxythiophene):poly(styrenesulfonate) hybrid solar cells. Nanotechnology, 2010, 21 (28), 285203

8. Rem S., Zhao N., Crawford S.C., Tambe M., Bulovic V., Gradečak S. Heterojunction Photovoltaics Using GaAs Nanowires and Conjugated Polymers Nano Lett. 2001, 11 (2), 408-413

9. Huang J., Miller P.F., Wilson J.S., de Mello A.J., de Mello J.C., Bradly D.D.C., Investigation of the Effects of Doping and Post-Deposition Treatments on the conductive, Morphology, and Work Function of Poly(3,4-ehtylenediosythiopehne)/Poly(styrene sulfonate) Films, Adv. Funct. Mater. 2005, 15, 1616-3028.

10. Price, M. J., Foley, J. M., May, R. A., Maldonado, S. Comparison of majority carrier charge transfer velocities at Si/polymer and Si/metal photovoltaic heterojunctions. Appl. Phys. Lett., 2010, 97, 083503

11. Lonergan M., Charge transport at conjugated polymer-inorganic semiconductor and conjugated polymer-metal interfaces, Annu. Rev. Phys. Chem., 2004, 55 (5), 257–98

12. Sze, S. M., Physics of Semiconductor Devices, New York: Wiley, 1981. Print.

12. Ritenour A.J., Cramer R.C., Levinrad S., Boettcher S.W., Efficient n-GaAs Photoelectrodes Grown by Close-Spaced Vapor Transport from a Solid-Course. ACS Appl. Mater. Interfaces, 2012, 4, 69-73.

13. Bessolov V.N., Lebedev M.V., Chalcogenide passivation of III-V semiconductor surfaces, Semiconductors, Semiconductors 1998, 32 (11), 1141-1156

14. Adlkofer K., Tanaka M., Hillebrand H., Wiegand G., Sackmann E., Bolom T., Deutschamann R., Abstreiter G., Electrochemical passivation of gallium arsenide surface with organic self-assembled monolayers in aqueous electrolytes, Appl. Phys. Lett., 2000, 76, 3313-3315

15. Lunt S.R., Santangelo P.G., Lewis N.S., Passivation of GaAs surface recombination with organic thiols, J. Vac. Sci. Technol. B, 1991, 9, 2333

16. Kim J.Y., Jung J.H., Lee D.E., Joo J., Enhancement of electrical conductivity of poly(3,4-ethylenedioxythiophene)/poly(4-styrenesulfonate) by a change of solvents, Synt. Met., 2002, 126, 311-316

17. Fan B., Mei X., Ouyang J., Significant Conductivity Enhancement of Conductive Poly(3,4-ethylenedioxythiophene: Poly(styrenesulfonate) Films by Addition of Anionic Surfactants into Polymer Solution, Macromolecules, 2008¸ 41, 5971-5973

18. Jones F.E., Daniels-Hafer C., Wood B.P., Danner R.G., Lonergan M.C., Current transport at the p-InP/poly(pyrrole) interface, J. Appl. Phys., 2001, 90, 1001

19 Missous M., Rhoderick E.H., Woolf D.A., Wilkes S.P., On the Richardson constant of intimate metal-GaAs Schottky barriers. Semicond. Sci. Technol., 1992, 7, 218

20. Julian C. C., Physics of Solar Energy, Wiley, 2011, 189

21. Yu T. H., Yan L., You W., Laghumavarapu R. B., Huffaker D., Ratsch C. The effect of passivation on different GaAs surfaces, 2013, 103, 173902

22. Mattoni A., Filippetti A., Hybrid perovskites for photovoltaics: Insights from first principles, Phys. Rev. B, 2014, 89, 125203

23. He M., Zheng D., Wang M., Lin C., Lin Z., High efficiency perovskite solar cells: from complex nanostructure to planer heterojunction, 2014, 2, 2994-6003